

## Electrochemical Properties of $\text{La}_4\text{Ni}_3\text{O}_{10}$ -GDC Composite Cathode by Facile Sol-gel Method for IT-SOFCs

Sihyuk Choi and Guntae Kim<sup>†</sup>

Department of Energy Engineering, Ulsan National Institute of Science and Technology (UNIST), Ulsan 689-798, Korea

(Received June 13, 2014; Revised July 17, 2014; Accepted July 18, 2014)

### ABSTRACT

Among the Ruddlesden-Popper series,  $\text{La}_4\text{Ni}_3\text{O}_{10}$  has received widespread attention as a promising cathode material by reason of its favorable properties for realizing high performance of intermediate temperature solid oxide fuel cells (IT-SOFCs). The  $\text{La}_4\text{Ni}_3\text{O}_{10}$  cathode is prepared using the facile sol-gel method by employing tri-blockcopolymer (F127) to obtain a single phase in a short sintering time. There are no reactions between the  $\text{La}_4\text{Ni}_3\text{O}_{10}$  cathode and the  $\text{Ce}_{0.9}\text{Gd}_{0.1}\text{O}_{2.5}$  (GDC) electrolyte upon sintering at 1000°C, indicating that the  $\text{La}_4\text{Ni}_3\text{O}_{10}$  cathode has good chemical compatibility with the GDC electrolyte. The maximum electrical conductivity of  $\text{La}_4\text{Ni}_3\text{O}_{10}$  reaches approximately  $240 \text{ S cm}^{-1}$  at 100°C and gradually decreases with increasing temperature in air atmosphere. The area specific resistance value of  $\text{La}_4\text{Ni}_3\text{O}_{10}$  composite with 40 wt% GDC is  $0.435 \Omega \text{ cm}^2$  at 700°C. These data allow us to propose that the  $\text{La}_4\text{Ni}_3\text{O}_{10}$ -GDC composite cathode is a good candidate for IT-SOFC applications.

**Key words :** Solid oxide fuel cell, Cathode, Ruddlesden-Popper, Tri-blockcopolymer (F127)

### 1. Introduction

Solid oxide fuel cells (SOFCs) are widely viewed as a promising source of power generation with very high efficiency, high power density, low emissions, and excellent fuel flexibility at high operating temperatures ( $>1000^\circ\text{C}$ ).<sup>1-4</sup> Even with the many benefits of SOFC technology, the necessary high operating temperature results in a number of problems such as high cost, electrode sintering, interface reactions between cell components, and material compatibility challenges. In this regard, many studies have been devoted to the development of intermediate-temperature (600-800°C) SOFCs (IT-SOFCs) as a way to reduce fabrication costs, improve long-term performance, and extend the range of applicable cell materials. However, there are major problems in the practical use of IT-SOFCs, including poor oxide-ion conductivity and the inadequate catalytic activity of conventional cathodes due to reduced operating temperature.<sup>5-8</sup> Therefore, the development of a new cathode material could be a key step toward the commercialization of IT-SOFCs.

In this respect, mixed oxide-ion and electronic conducting (MIEC) oxides, containing Mn, Fe, Co, and/or Ni with perovskite structures, have been studied extensively as alternative cathode materials.<sup>9-11</sup> Among the various MIEC oxides, cobalt containing oxides have attracted strong interest owing to their high electrocatalytic activity for the oxy-

gen reduction reaction (ORR). In spite of their excellent properties, cobalt-containing oxides exhibit high thermal expansion coefficients (TECs) and easy evaporation of cobalt (Co).<sup>12,13</sup>

Alternatively, Co-free  $\text{La}_2\text{NiO}_4$  has received significant attention as a mixed conductor material derived from  $\text{K}_2\text{NiF}_4$ -type materials for IT-SOFC cathodes by reason of its important advantages including relatively high oxygen ionic conductivity, attractive electronic conductivity, moderate TECs, and high electrocatalytic activity under oxidizing conditions.<sup>14-16</sup>  $\text{La}_2\text{NiO}_4$  is the first member of the Ruddlesden-Popper homologous series; materials in this series have a general formula  $\text{La}_{n+1}\text{Ni}_n\text{O}_{3n+1}$ , where  $n$  represents the number of perovskite layers in a formula unit. The Ruddlesden-Popper structure can be described as having alternating perovskite layers ( $\text{LaNiO}_3$ ) <sub>$n$</sub>  and rock-salt layers (LaO) along the crystallographic  $c$  direction, as shown Fig. 1. The number of perovskite layers increases with increasing  $n$  in this structure, leading to the formation of the higher order Ruddlesden-Popper phases,  $\text{La}_3\text{Ni}_2\text{O}_7$  and  $\text{La}_4\text{Ni}_3\text{O}_{10}$ , which show faster ionic and electronic transport properties.<sup>17-20</sup> These effects are primarily related with the increasing concentration of Ni-O-Ni bonds, which are responsible for electronic conduction, progressive delocalization of p-type electronic charge carriers, and increasing vacancy-migration contribution to oxygen ion diffusivity.

Recently, Amow *et al.* performed impedance spectroscopy analyses of  $\text{La}_{n+1}\text{Ni}_n\text{O}_{3n+1}$  ( $n = 1, 2, \text{ and } 3$ ) symmetrical cells on  $\text{La}_{0.9}\text{Sr}_{0.1}\text{Ga}_{0.8}\text{Mg}_{0.2}\text{O}_{3-\delta}$  (LSGM) electrolyte; they found that the area specific resistance (ASR) decreases with increasing  $n$ , which was attributed to increasing electrical conductivity.<sup>17</sup> Furthermore, our group carried out the

<sup>†</sup>Corresponding author : Guntae Kim

E-mail : gtkim@unist.ac.kr

Tel : +82-52-217-2917 Fax : +82-52-217-2909

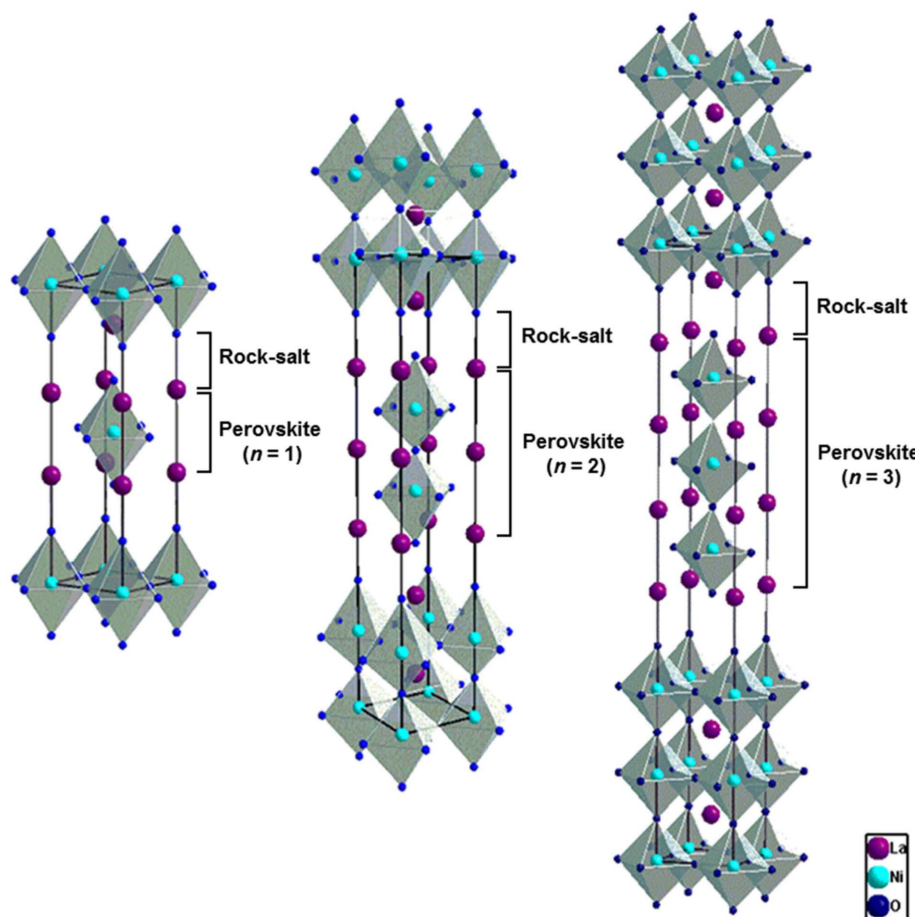


Fig. 1. The crystal structure of  $\text{La}_{n+1}\text{Ni}_n\text{O}_{3n+1}$  ( $n = 1, 2, \text{ and } 3$ ).

preparation of  $\text{La}_{n+1}\text{Ni}_n\text{O}_{3n+1}$  ( $n = 1, 2, \text{ and } 3$ )-YSZ composite using the infiltration method.<sup>20)</sup> The electrical conductivity and electrochemical performance were enhanced with increasing  $n$ , which is the electronic conducting perovskite layer. As a consequence,  $\text{La}_4\text{Ni}_3\text{O}_{10}$  is the most favorable cathode material for IT-SOFC applications.

To achieve a single phase of  $\text{La}_4\text{Ni}_3\text{O}_{10}$ , many groups have recently employed various synthesis methods such as the Pechini method, solid state reaction, and the hydrothermal method. However, using those methods, the preparation of  $\text{La}_4\text{Ni}_3\text{O}_{10}$  requires multiple processes and long sintering time. For example,  $\text{La}_4\text{Ni}_3\text{O}_{10}$  was synthesized by the Amow group using the Pechini method, which required sintering at  $1050^\circ\text{C}$  for 6 days with one intermittent regrinding step.<sup>17)</sup> Furthermore, Zhang *et al.* prepared  $\text{La}_4\text{Ni}_3\text{O}_{10}$  by calcination at  $1100^\circ\text{C}$  for 4 ~ 5 days in air, also with several grinding processes.<sup>18)</sup>

With the aim of reducing the time for material synthesis, we present a facile method for the synthesis of pure phase  $\text{La}_4\text{Ni}_3\text{O}_{10}$  oxide obtained by employing tri-blockcopolymer (F127) as a chelating agent. Tri-blockcopolymer (F127) is a poly (ethylene oxide)–poly (propylene oxide)–poly (ethylene oxide); it is used as a structure-directing agent in the syn-

thesis of ordered mesoporous materials based on the PEO-metal complexation.<sup>21)</sup> This paper focuses on the synthesis of pure phased  $\text{La}_4\text{Ni}_3\text{O}_{10}$  using the sol-gel method; in terms of future application of this material as an IT-SOFC cathode material, we focus on the structural characteristics, electrical properties, and electrochemical performances of pure phased  $\text{La}_4\text{Ni}_3\text{O}_{10}$  based on a  $\text{Ce}_{0.9}\text{Gd}_{0.1}\text{O}_{2-\delta}$  (GDC) electrolyte.

## 2. Experimental Procedure

$\text{La}_4\text{Ni}_3\text{O}_{10}$  powder was synthesized using the sol-gel process with stoichiometric amounts of  $\text{La}(\text{NO}_3)_3 \cdot 6\text{H}_2\text{O}$  (Aldrich, 99.9%),  $\text{Ni}(\text{NO}_3)_2 \cdot 6\text{H}_2\text{O}$  (Aldrich), and F127 (Aldrich). F127 was dissolved in distilled water and nitrate salts were added. The homogeneous sol was dried in a dry oven at  $100^\circ\text{C}$  to form a gel. After drying, the gel was heated to  $300^\circ\text{C}$ ; then, the primary powder was formed via a combustion reaction. This powder was ball-milled in acetone for 24 h and then sintered at  $1100^\circ\text{C}$  for 12 h in air to form a single phase. For measurement of the cell performances of  $\text{La}_4\text{Ni}_3\text{O}_{10}$  powder, slurries consisting of powders, GDC, and an organic binder (Heraeus V006) were used at a weight ratio of 6 : 4 : 12.

The phase identification of  $\text{La}_4\text{Ni}_3\text{O}_{10}$  was confirmed by X-ray powder diffraction (XRD) (Rigaku-diffractometer, Cu K $\alpha$  radiation) with a scanning rate of  $0.5^\circ \text{ min}^{-1}$  in the  $2\theta$  range of 20 to  $80^\circ$ . The microstructures of the interface between the GDC electrolyte and the  $\text{La}_4\text{Ni}_3\text{O}_{10}$  cathode were examined using a field emission scanning electron microscope (FE-SEM) (Nova SEM). The electrical conductivity of the  $\text{La}_4\text{Ni}_3\text{O}_{10}$  cathode was evaluated using a four-terminal DC arrangement; a potentiostat (BioLogic) was used to measure the current and voltage at intervals of  $50^\circ\text{C}$  at temperatures ranging from 100 to  $750^\circ\text{C}$ .

Electrochemical impedance spectroscopy of the  $\text{La}_4\text{Ni}_3\text{O}_{10}$  cathode was performed using a symmetrical cell. The GDC electrolyte powders were pressed into pellets and then sintered at  $1350^\circ\text{C}$  for 4 h in air to obtain a dense electrolyte substrate. The slurry composed of  $\text{La}_4\text{Ni}_3\text{O}_{10}$ -GDC powder was screen-printed onto both sides of the GDC electrolytes to form symmetrical half-cells; this was followed by calcination at  $1000^\circ\text{C}$  for 4 h. A silver paste was used as a current collector for the electrodes. Impedance spectra were recorded under open circuit voltage (OCV) in a frequency range of 1 MHz to 500 kHz with AC perturbation of 14 mV from 600 to  $750^\circ\text{C}$ .

### 3. Results and Discussion

Figure 2 shows the XRD pattern of the  $\text{La}_4\text{Ni}_3\text{O}_{10}$  cathode synthesized via the sol-gel process after heat treatment at  $1100^\circ\text{C}$  for 12 h in air. The pattern reveals a single-phase material exhibiting an orthorhombic structure without any impurity phase, as has been identified in other studies. It was also necessary to investigate the chemical compatibility between the  $\text{La}_4\text{Ni}_3\text{O}_{10}$  cathode and the GDC electrolyte because the phase reaction between the electrode and the electrolyte can cause the formation of an undesired insulating layer at the interface, which would block oxide-ionic and electronic transport.<sup>22)</sup> The chemical reactivity of the  $\text{La}_4\text{Ni}_3\text{O}_{10}$ -GDC composite was confirmed after sintering at

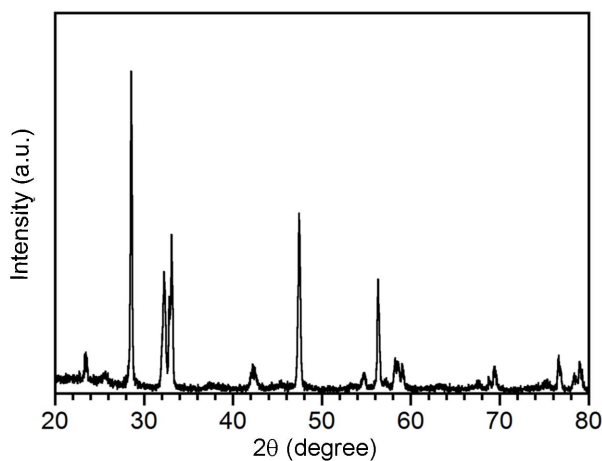


Fig. 2. X-ray diffraction pattern for  $\text{La}_4\text{Ni}_3\text{O}_{10}$  powder after heat treatment at  $1100^\circ\text{C}$  for 12 h in air.

$1000^\circ\text{C}$  for 4 h by mixing the corresponding powders at a weight ratio of 6 : 4. As indicated in Fig. 3, there are no obvious reactions between  $\text{La}_4\text{Ni}_3\text{O}_{10}$  and GDC upon sintering at  $1000^\circ\text{C}$ ; the patterns indicate that the  $\text{La}_4\text{Ni}_3\text{O}_{10}$  cathode has good chemical compatibility with the GDC electrolyte.

A cross-sectional SEM image of the  $\text{La}_4\text{Ni}_3\text{O}_{10}$ -GDC composite cathode is provided in Fig. 4. The bottom image represents the microstructure of the dense GDC electrolyte; the upper image represents the microstructure of the porous cathode  $\text{La}_4\text{Ni}_3\text{O}_{10}$ -GDC composite after sintered at  $1000^\circ\text{C}$ . The dense GDC electrolyte adheres very well to the porous composite cathode layer, without cracks, indicating the good compatibility between the electrolyte and the electrode. The thicknesses of the electrolyte and the cathode layer are approximately 800 and 20  $\mu\text{m}$ , respectively.

Figure 5 shows the temperature dependence of the electrical conductivity of  $\text{La}_4\text{Ni}_3\text{O}_{10}$  in air. The maximum electrical

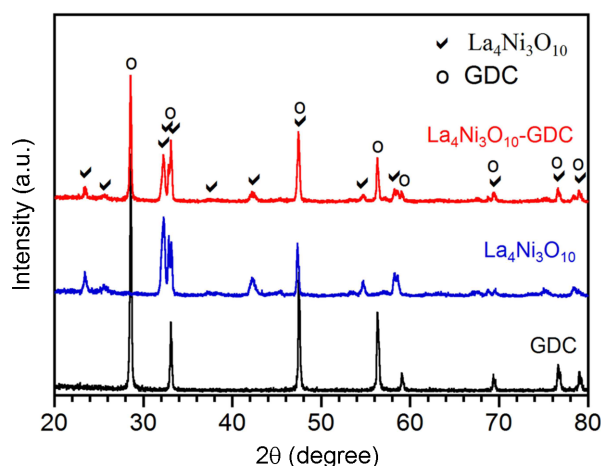


Fig. 3. X-ray diffraction pattern of  $\text{La}_4\text{Ni}_3\text{O}_{10}$  and GDC mixture sintered at  $1000^\circ\text{C}$  for 4 h in air.

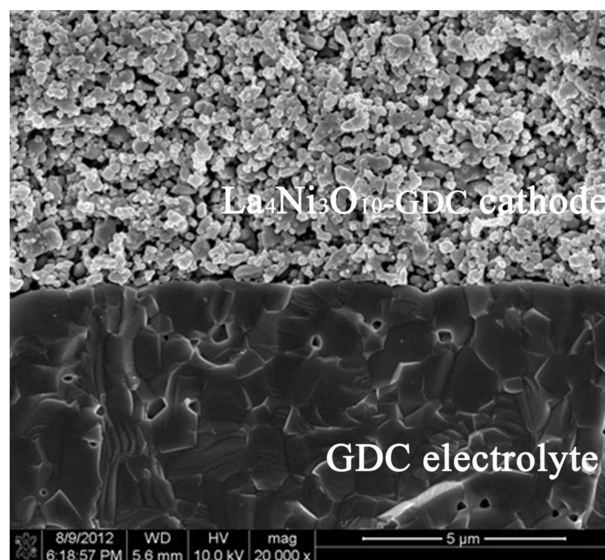
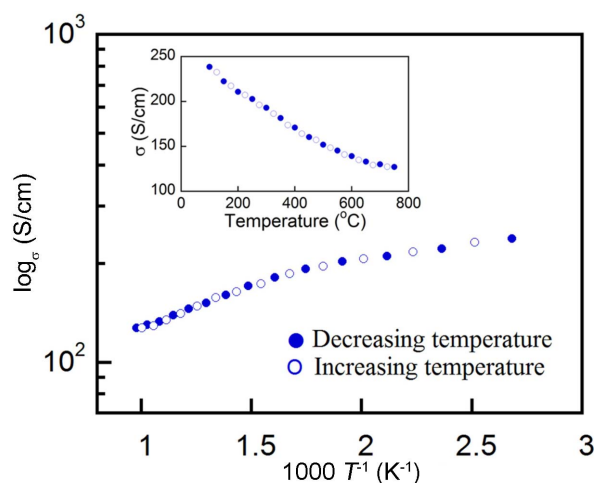


Fig. 4. Cross-sectional SEM image of  $\text{La}_4\text{Ni}_3\text{O}_{10}$ -GDC cathode and GDC electrolyte interface.



**Fig. 5.** The electrical conductivity of  $\text{La}_4\text{Ni}_3\text{O}_{10}$  in air as a function of temperature, open and closed symbols correspond to measurements on heating and cooling.

conductivity of  $\text{La}_4\text{Ni}_3\text{O}_{10}$  reaches approximately  $240 \text{ S cm}^{-1}$  at  $100^\circ\text{C}$  and gradually decreases with increasing temperature, exhibiting metallic conduction behavior over the whole temperature range. For an SOFC cathode material, the electrical conductivity should be higher than  $100 \text{ S cm}^{-1}$  at the operating temperature.<sup>23)</sup> The lowest electrical conductivity of  $\text{La}_4\text{Ni}_3\text{O}_{10}$  at  $750^\circ\text{C}$  is about  $130 \text{ S cm}^{-1}$ , which is adequate for the sample to be employed as a cathode in IT-SOFCs.

The electrocatalytic activity for the oxygen reduction reaction of a cathode can be obtained by performing electrochemical impedance spectroscopy (EIS) measurement on  $\text{La}_4\text{Ni}_3\text{O}_{10}$ -GDC/GDC/ $\text{La}_4\text{Ni}_3\text{O}_{10}$ -GDC symmetrical cell. The cathodic polarization resistance, normalized by the geometric electrode area, that is, the area specific resistance (ASR), can be calculated from the impedance spectra acquired under open circuit conditions. When the electronic conduction in the electrolyte is negligible, the cathodic polarization resistance can be adequately approximated using the diameter of the impedance loop or the difference between the high-frequency and low-frequency intercepts at the real axis, as presented in Fig. 6(a). The ASR values of the  $\text{La}_4\text{Ni}_3\text{O}_{10}$ -GDC composite based on the GDC electrolyte are  $0.207$ ,  $0.435$ ,  $1.066$ , and  $2.432 \text{ } \Omega \text{ cm}^2$  at  $750$ ,  $700$ ,  $650$ , and  $600^\circ\text{C}$ , respectively. These values are comparable to those reported for other conventional SOFC cathode materials, such as the value of  $0.75 \text{ } \Omega \text{ cm}^2$  at  $700^\circ\text{C}$  for an  $\text{La}_{0.8}\text{Sr}_{0.2}\text{MnO}_3$ -GDC composite based on GDC electrolyte.<sup>24)</sup>

The impedance spectra are fitted well to the equivalent circuit, as can be seen in the inset of Fig. 6(a) and as is summarized in Table 1. In the equivalent circuit,  $L$  is the inductance induced by the cables. The real axis value at the high frequency intercepts,  $R_1$ , mainly correspond to the electrolyte and wire resistances. In the Nyquist plots, high-frequency arcs are equivalent to  $R_2$ , which is caused by charge transfer during the migration and diffusion of oxygen ions

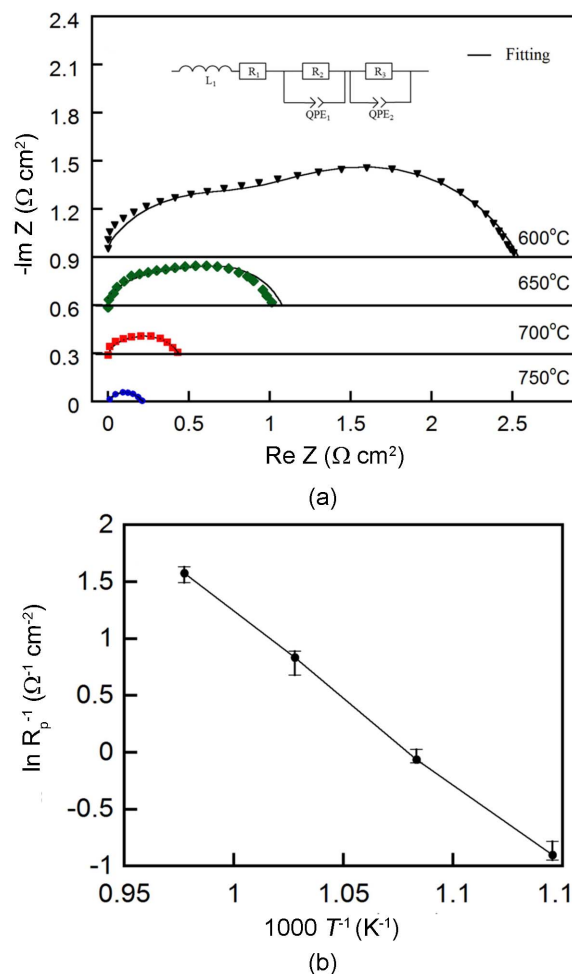


**Fig. 6.** (a) Impedance spectra and fitted Nyquist plots of  $\text{La}_4\text{Ni}_3\text{O}_{10}$ -GDC cathode on GDC electrolyte in symmetrical cell measured under OCV condition. (b) Arrhenius plot of the polarization resistance of  $\text{La}_4\text{Ni}_3\text{O}_{10}$ -GDC cathode.

**Table 1.** Fitting Result of  $\text{La}_4\text{Ni}_3\text{O}_{10}$ -GDC Composite with Different Temperatures

T ( $^\circ\text{C}$ )	750	700	650	600
L (H)	$2.51 \times 10^{-7}$	$2.45 \times 10^{-7}$	$1.98 \times 10^{-7}$	$1.66 \times 10^{-7}$
$R_1$ ( $\Omega \text{ cm}^2$ )	1.273	1.696	2.251	3.320
$R_2$ ( $\Omega \text{ cm}^2$ )	0.242	0.337	0.612	1.114
$R_3$ ( $\Omega \text{ cm}^2$ )	0.008	0.123	0.538	1.540

from the TPB to the electrolyte lattice. Meanwhile, low-frequency arcs correspond to  $R_3$ , which is associated with the adsorption/desorption of molecular oxygen and the diffusion of bulk or surface oxygen.<sup>25)</sup> From the data,  $R_3$  can be seen to be the more prevailing factor than  $R_2$  with decreasing temperature. Consequently,  $R_3$  can be regarded as a rate determining step in the  $\text{La}_4\text{Ni}_3\text{O}_{10}$ -GDC composite system.

The temperature dependence of ASR on the  $\text{La}_4\text{Ni}_3\text{O}_{10}$ -GDC composite is illustrated by the Arrhenius plot shown in Fig. 6(b). The apparent activation energy ( $E_a$ ) of the

La<sub>4</sub>Ni<sub>3</sub>O<sub>10</sub>-GDC was calculated and found to be 123 kJ mol<sup>-1</sup>, which is close to that of a Ba<sub>0.5</sub>Sr<sub>0.5</sub>Co<sub>0.8</sub>Fe<sub>0.2</sub>O<sub>3-δ</sub> cathode (116 kJ mol<sup>-1</sup>) on samarium doped ceria electrolyte, as reported by Shao *et al.*<sup>5)</sup> It is obvious that the La<sub>4</sub>Ni<sub>3</sub>O<sub>10</sub>-GDC cathode has high activity for the oxygen reduction reaction. Therefore, the La<sub>4</sub>Ni<sub>3</sub>O<sub>10</sub>-GDC composite derived using the facile sol-gel method by employing tri-blockcopolymer (F127) can be considered acceptable as an IT-SOFC.

#### 4. Conclusions

La<sub>4</sub>Ni<sub>3</sub>O<sub>10</sub> is chosen as a base material by reason of its favorable properties for realizing high performance of intermediate temperature solid oxide fuel cells (IT-SOFCs). In order to reduce the time required to synthesize the La<sub>4</sub>Ni<sub>3</sub>O<sub>10</sub> cathode, the facile sol-gel method is employed using tri-blockcopolymer (F127). A single phase of La<sub>4</sub>Ni<sub>3</sub>O<sub>10</sub> is obtained after heat treatment at 1100°C for 12 h in air. There are no reactions between La<sub>4</sub>Ni<sub>3</sub>O<sub>10</sub> and GDC upon sintering at 1000°C, indicating that the La<sub>4</sub>Ni<sub>3</sub>O<sub>10</sub> cathode has good chemical compatibility with the GDC electrolyte. The maximum electrical conductivity of La<sub>4</sub>Ni<sub>3</sub>O<sub>10</sub> reaches approximately 240 S cm<sup>-1</sup> at 100°C and gradually decreases with increasing temperature in air atmosphere. The area specific resistance value of the La<sub>4</sub>Ni<sub>3</sub>O<sub>10</sub> composite with 40 wt% GDC is 0.435 Ω cm<sup>2</sup> at 700°C. These data allow us to propose that the La<sub>4</sub>Ni<sub>3</sub>O<sub>10</sub>-GDC composite based on GDC electrolyte, considering its electrical properties and electrochemical performance, is a preferable candidate cathode material in IT-SOFC applications.

#### Acknowledgment

This research was supported by the Brain Korea 21 plus (10Z2013001105), funded through the Korean Government Ministry of Education.

#### REFERENCES

1. B. C. H. Steele and A. Heinzl, "Materials for Fuel-cell Technologies," *Nature*, **414** 345-52 (2001).
2. S. Park, J. M. Vohs, and R. J. Gorte, "Direct Oxidation of Hydrocarbons in a Solid Oxide Fuel Cell," *Nature*, **404** 265-67 (2000).
3. M. Liu, M. E. Lynch, K. Blinn, F. M. Alamgir, and Y. Choi, "Rational SOFC Material Design: New Advances and Tools," *Mater. Today*, **14** [11] 534-46 (2011).
4. Z. Shao, S. M. Haile, J. Ahn, P. D. Ronney, Z. Zhan, and S. A. Barnett, "A Thermally Self-sustained Micro Solid-oxide Fuel-cell Stack with High Power Density," *Nature*, **435** 795-98 (2005).
5. Z. Shao and S. M. Haile, "A High-performance Cathode for the Next Generation of Solid Oxide Fuel Cells," *Nature*, **431** 170-73 (2004).
6. S. Choi, S. Yoo, J. Kim, S. Park, A. Jun, S. Sengodan, J. Kim, J. Shin, H. Y. Jeong, Y. Choi, G. Kim, and M. Liu, "Highly Efficient and Robust Cathode Materials for Low-temperature Solid Oxide Fuel Cells: PrBa<sub>0.5</sub>Sr<sub>0.5</sub>Co<sub>2-x</sub>Fe<sub>x</sub>O<sub>5+δ</sub>," *Sci. Rep.*, **3** 2426 (2013).
7. S. Choi, J. Shin, K. M. Ok, and G. Kim, "Chemical Compatibility, Redox Behavior, and Electrochemical Performance of Nd<sub>1-x</sub>Sr<sub>x</sub>CoO<sub>3-δ</sub> Cathodes Based on Ce<sub>1.9</sub>Gd<sub>0.1</sub>O<sub>1.95</sub> for Intermediate-temperature Solid Oxide Fuel Cells," *Electrochim. Acta.*, **81** 217-23 (2012).
8. S. Park, S. Choi, J. Shin, and G. Kim, "Electrochemical Investigation of Strontium Doping Effect on High Performance Pr<sub>1-x</sub>Sr<sub>x</sub>CoO<sub>3-δ</sub> (x = 0.1, 0.3, 0.5, and 0.7) Cathode for Intermediate-temperature Solid Oxide Fuel Cells," *J. Power Sources*, **210** 172-77 (2012).
9. J. H. Kim, M. Cassidy, J. T. S. Irvine, and J. Bae, "Electrochemical Investigation of SmBa<sub>0.5</sub>Sr<sub>0.5</sub>Co<sub>2</sub>O<sub>5+δ</sub> Composite Cathodes with Cathodes for Intermediate Temperature-operating Solid Oxide Fuel Cells," *Chem. Mater.*, **22** 883-92 (2010).
10. G. Kim, S. Wang, A. J. Jacobson, L. Reimus, P. Brodersen, and C. A. Mims, "Rapid Oxygen Ion Diffusion and Surface Exchange Kinetics in PrBaCo<sub>2</sub>O<sub>5+x</sub> with a Perovskite-related Structure and Ordered a Cations," *J. Mater. Chem.*, **17** 2500-05 (2007).
11. S. Park, S. Choi, J. Shin, and G. Kim, "A Collaborative Study of Sintering and Composite Effects for a PrBa<sub>0.5</sub>Sr<sub>0.5</sub>Co<sub>2-x</sub>Fe<sub>x</sub>O<sub>5+δ</sub> IT-SOFC Cathode," *RSC Adv.*, **4** 1775-81 (2014).
12. A. Jun, J. Shin, and G. Kim, "High Redox and Performance Stability of Layered SmBa<sub>0.5</sub>Sr<sub>0.5</sub>Co<sub>1.5</sub>Cu<sub>0.5</sub>O<sub>5+δ</sub> Perovskite Cathodes for Intermediate-temperature Solid Oxide Fuel Cells," *Phys. Chem. Chem. Phys.*, **15** [45] 19906-12 (2013).
13. S. Park, S. Choi, J. Shin, and G. Kim, "Tradeoff Optimization of Electrochemical Performance and Thermal Expansion for Co-based Cathode Material for Intermediate-temperature Solid Oxide Fuel Cells," *Electrochim. Acta*, **125** 683-90 (2014).
14. V. V. Kharton, A. P. Viskup, E. N. Naumovich, and F. M. B. Marques, "Oxygen Ion Transport in La<sub>2</sub>NiO<sub>4</sub>-based Ceramics," *J. Mater. Chem.*, **9** [10] 2623-29 (1999).
15. V. V. Kharton, A. V. Kovalevsky, M. Avdeev, E. V. Tsipis, M. V. Patrakeev, A. A. Yaremchenko, E. N. Naumovich, and J. R. Frade, "Chemically Induced Expansion of La<sub>2</sub>NiO<sub>4-δ</sub>-based Materials," *Chem. Mater.*, **19** 2027-33 (2007).
16. J. A. Kilner and C. K. M. Shaw, "Mass Transport in La<sub>2</sub>Ni<sub>1-x</sub>Co<sub>x</sub>O<sub>4+δ</sub> Oxides with the K<sub>2</sub>NiF<sub>4</sub> Structure," *Solid State Ionics*, **154** 523-27 (2002).
17. G. Amow, I. J. Davidson, and S. J. Skinner, "A Comparative Study of the Ruddlesden-Popper Series, La<sub>n+1</sub>Ni<sub>n</sub>O<sub>3n+1</sub> (n = 1, 2, and 3), for Solid-oxide Fuel-cell Cathode Applications," *Solid State Ionics*, **177** [13-14] 1205-10 (2006).
18. Z. Zhang and M. Greenblatt, "Synthesis, Structure, and Properties of Ln<sub>4</sub>Ni<sub>3</sub>O<sub>10-δ</sub> (Ln = La, Pr, and Nd)," *J. Solid State Chem.*, **117** [2] 236-46 (1995).
19. V. V. Kharton, A. A. Yaremchenko, and E. N. Naumovich, "Research on the Electrochemistry of Oxygen Ion Conductors in the Former Soviet Union. II. Perovskite-related Oxides," *J. Solid State Electrochem.*, **3** [6] 303-26 (1999).
20. S. Choi, S. Yoo, J. Y. Shin, and G. Kim, "High Performance SOFC Cathode Prepared by Infiltration of La<sub>n+1</sub>Ni<sub>n</sub>O<sub>3n+1</sub> (n = 1, 2, and 3) in Porous YSZ," *J. Electrochem. Soc.*, **158** [8]

- B995-99 (2011).
21. P. Yang, D. Zhao, D. I. Margolese, B. F. Chmelka, and G. D. Stucky, "Generalized Syntheses of Large-pore Mesoporous Metal Oxides with Semicrystalline Frameworks," *Nature*, **396** 152-55 (1998).
22. C. Rossignol, J. M. Ralph, J. M. Bae, and J. T. Vaughey, " $\text{Ln}_{1-x}\text{Sr}_x\text{CoO}_3$  (Ln=Gd, Pr) as a Cathode for Intermediate-temperature Solid Oxide Fuel Cells," *Solid State Ionics*, **175** [1-4] 59-61 (2004).
23. E. Boehm, J. M. Bassat, M. C Steil, P. Dordoe, F. Mauvy, and J. C. Grenier, "Oxygen Transport Properties of  $\text{La}_2\text{Ni}_{1-x}\text{Cu}_x\text{O}_{4+\delta}$  Mixed Conducting Oxides," *Solid State Sci.*, **5** [7] 973-81 (2003).
24. E. P. Murray and S. A. Barnett, "(La,Sr)MnO<sub>3</sub>-(Ce,Gd)O<sub>2-x</sub> Composite Cathodes for Solid Oxide Fuel Cells," *Solid State Ionics*, **143** [3-4] 265-73 (2001).
25. S. B. Adler, X. Y. Chen, and J. R. Wilson, "Mechanisms and Rate Laws for Oxygen Exchange on Mixed-conducting Oxide Surfaces," *J. Catal.*, **245** [1] 91-109 (2007).